5760 *Biochemistry* **2009,** *48,* 5760–5768
DOI: 10.1021/bi9004232

BIOCHEMISTRY
including biophysical chemistry & molecular biology
Article

Induced Fit and Equilibrium Dynamics for High Catalytic Efficiency in Ferredoxin-NADP(H) Reductases[†]

Darío H. Paladini, Matías A. Musumeci, Néstor Carrillo, and Eduardo A. Ceccarelli*

Molecular Biology Division, Instituto de Biología Molecular y Celular de Rosario (IBR), CONICET, Facultad de Ciencias Bioquímicas y Farmacéuticas, Universidad Nacional de Rosario, Suipacha 531, S2002LRK Rosario, Argentina

Received November 14, 2008; Revised Manuscript Received April 29, 2009

ABSTRACT: Ferredoxin-NADP(H) reductase (FNR) is a FAD-containing protein that catalyzes the reversible transfer of electrons between NADP(H) and ferredoxin or flavodoxin. This enzyme participates in the redox-based metabolism of plastids, mitochondria, and bacteria. Plastidic plant-type FNRs are very efficient reductases in supporting photosynthesis. They have a strong preference for NADP(H) over NAD(H), consistent with the main physiological role of $NADP^+$ photoreduction. In contrast, FNRs from organisms with heterotrophic metabolisms or anoxygenic photosynthesis display turnover rates that are up to 100-fold lower than those of their plastidic and cyanobacterial counterparts. With the aim of elucidating the mechanisms by which plastidic enzymes achieve such high catalytic efficiencies and NADP(H) specificity, we investigated the manner in which the NADP(H) nicotinamide enters and properly binds to the catalytic site. Analyzing the interaction of different nucleotides, substrate analogues, and aromatic compounds with the wild type and the mutant Y308S-FNR from pea, we found that the interaction of the 2′-P-AMP moiety from $NADP^+$ induces a change that favors the interaction of the nicotinamide, thereby facilitating the catalytic process. Furthermore, the main role of the terminal tyrosine, Y308, is to destabilize the interaction of the nicotinamide with the enzyme, inducing product release and favoring discrimination of the nucleotide substrate. We determined that this function can be replaced by the addition of aromatic compounds that freely diffuse in solution and establish a dynamic equilibrium, reversing the effect of the mutation in the Y308S-FNR mutant.

Photosynthesis is one of the most energetically significant biological processes on earth. An important and limiting step of this process involves electron transfer via ferredoxin (Fd)[1] from photosystem I to $NADP^+$; this step is catalyzed by ferredoxin (flavodoxin)-NADP(H) oxidoreductase (FNR, EC 1.18.1.2). FNRs utilize a noncovalently bound FAD cofactor as a redox center which functions as a general electronic splitter, transferring electrons between obligatory one- and two-electron carriers (*1*, *2*), as is often the case in other flavoenzymes.

In nonphototrophic bacteria and eukaryotes, FNR mainly works in the direction opposite from that of photosynthesis, providing reducing power in the form of Fd and flavodoxin for use in multiple metabolic pathways, such as steroid hydroxylation in mammalian mitochondria, as well as nitrite reduction and glutamate synthesis in heterotrophic tissues of vascular plants (for reviews, see refs (*1*) and (*2*)).

Since plastidic FNRs mediate a rate-limiting step of photosynthesis, they have been forced to evolve to highly catalytic efficient enzymes relative to their bacterial counterparts, which are ~20−100-fold less active. Turnover rates in the range of 200−600 s^{-1} have been reported for *Chlamydomonas reinhardtii*, *Anabaena*, and plant FNRs (*2*). In contrast, bacterial reductases exhibit low efficiency which is primarily attributable to a severe reduction in k_{cat} values without significant changes in the K_m values for all substrates (*2*). Another aspect of these enzymes that has been well studied is their extraordinary preference for NADP(H) over NAD(H) (*3*, *4*). However, the molecular grounds for the catalytic efficiency and substrate discrimination in plastidic FNRs are not well understood, and no conclusive correlation between enzyme structure and catalytic mechanism has been determined. FNRs contain two domains: an antiparallel β-barrel that comprises the FAD binding core, at the amino terminus of the flavoprotein, and a carboxyl-terminal domain involved in NADP(H) binding, with a characteristic α-helix−β-strand fold (*5*). Previous studies indicate that the terminal tyrosine (Y308 in pea FNR) may be responsible in part for substrate specificity (*6*, *7*). This residue is conserved in all plant-type FNRs, is stacked coplanar to the *re*-face of the isoalloxazine moiety, and makes extensive interactions with it (*1*, *2*, *5*, *8*) (Figure 1A). The stacking of the terminal tyrosine onto the isoalloxazine ring system may weaken the interaction between the nicotinamide and the prosthetic group, thereby increasing the degree of discrimination between NADP(H) and NAD(H) due to the extra phosphate group. As a result of these interactions, a decrease in the binding

[†]This work was supported by grants from CONICET and the Agencia de Promoción Científica y Tecnológica (ANPCyT, Argentina).

*To whom correspondence should be addressed: IBR, CONICET, Facultad de Ciencias Bioquímicas y Farmacéuticas, UNR, Suipacha 531, S2002LRK Rosario, Argentina. Fax: +54 341 4390465. Telephone: +54 341-4351235. E-mail: ceccarelli@ibr.gov.ar.

[1]Abbreviations: FNR, ferredoxin (flavodoxin)-NADP(H) reductase; Fd, ferredoxin; DMAP, *N*,*N*-dimethyl-4-aminopyridine; NMNH, nicotinamide mononucleotide.

 Published on Web 05/12/2009 © 2009 American Chemical Society

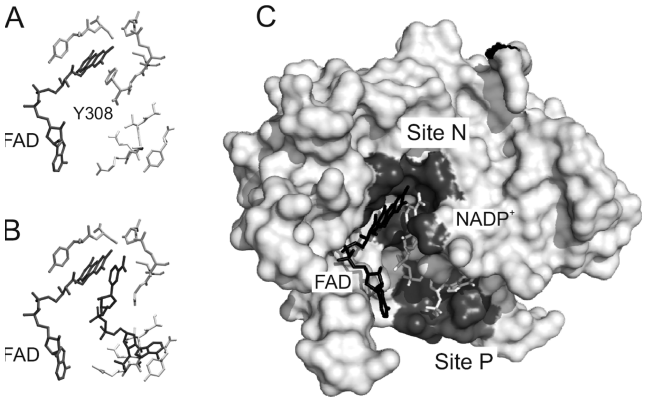

FIGURE 1: Nucleotide binding site of ferredoxin-NADP(H) reductase: (A) view of amino acid neighbors and the prosthetic group FAD at the NADP(H) binding site of pea FNR, (B) view of NADP(H) bound to the Y308S-FNR mutant (FAD and $NADP^+$ are depicted in black), and (C) surface model of pea Y308S-FNR containing bound $NADP^+$. Sites N and P are colored dark gray; FAD is colored black and $NADP^+$ light gray. The models are based on Protein Data Bank entries 1QG0 and 1QFY (*9*). Panels A and B were drawn using Swiss-PdbViewer 3.7 and rendered with POV-Ray. Panel C was constructed with PyMOL version 0.99 from DeLano Scientific.

affinity for NADP(H) relative to those of the 2′-P-AMP and 2′-P-ADP-ribose analogues is observed (*6*, *9*, *10*).

During enzyme catalysis, the nicotinamide ring must be positioned in the proximity of the *re*-face of the isoalloxazine moiety to permit electron transfer between the cofactor and substrate, displacing in the process the aromatic side chain of the carboxyl-terminal tyrosine (*6*, *7*, *10*−*12*) (Figure 1B). Evidence that the mobility of the carboxyl-terminal backbone region of FNR (mainly the Y308 residue) is essential for obtaining an FNR enzyme with high catalytic efficiency has been recently obtained (*13*). Similarly, using NMR techniques, it has been demonstrated that the entire carboxyl-terminal region, including the tyrosine, is perturbed upon $NADP^+$ binding (*14*). These conformational changes could be responsible for the reciprocal negative cooperativity of binding between ferredoxin and $NADP^+$ and the positive cooperativity observed at the kinetic level (*15*, *16*). Conformational movements that occur upon nucleotide binding displace the NADP(H) binding domain slightly as a single unit, moving the E306 side chain (in pea FNR) within hydrogen bonding distance of the hydroxyl group of S96 (*17*), thereby optimizing the geometry for electron and hydride transfer. $NADP^+$ binds to FNR in a bipartite manner; i.e., the two moieties of the dinucleotide can bind to the enzyme in a partially independent way (*6*). The 2′-P-AMP portion first binds in a nonproductive conformation at site P. The NMN moiety then establishes a loosely bound complex that is compatible with turnover at site N (*9*) (see Figure 1C). The loop including C266, G267, and L268 (numbers as in pea FNR) has been proposed to undergo a structural rearrangement upon $NADP^+$ binding, influencing the catalytic efficiency of the enzyme and the fast exchange of NADP(H) (*8*, *18*).

In this work, we have studied the interaction of NADP(H) and different nucleotide analogues with wild-type pea FNR and the Y308S-FNR mutant. We have also analyzed the effect of aromatic compounds that can interact with site N and mimic the effect of the terminal tyrosine on the activity of the wild-type enzyme and Y308S-FNR mutant. Our findings allow us to propose that interaction of the 2′-P-AMP moiety from NADP(H) at site P induces a change in the interaction of the nicotinamide in site N. In contrast, interaction of the NADP(H) nicotinamide with site N does not affect binding of the NADP(H) 2′-P-AMP moiety to site P and is strongly influenced by the terminal amino acid, Y308 (see Figure 1). Interestingly, the function of Y308 during catalysis can be replaced "in trans" by addition of the aromatic compound *N*,*N*-dimethyl-4-aminopyridine (DMAP) in the Y308S-FNR mutant, largely reverting the effect of the mutation. Here we offer evidence that the high catalytic efficiency in FNRs is obtained by the concerted contribution of two processes thought to be independent: induced fit of the substrate by means of a conformational change as postulated by Koshland (*19*) and equilibrium dynamics in which the active moiety of the substrate binds to one of the possible preexisting conformations, as first introduced for allosteric enzymes by Monod et al. (*20*).

EXPERIMENTAL PROCEDURES

Plasmid Construction, Protein Expression, and Purification. Wild-type and mutant pea FNRs were expressed in *Escherichia coli* using pET205DP. This plasmid is derived from vector pET205 (*21*), which expresses a Trx-His-Tag-FNR fusion protein containing a thrombin recognition site between the His tag and the mature FNR. A kanamycin resistance marker cassette was introduced into pET205 to improve stability during protein expression, resulting in pET205DP. The pea Y308S-FNR mutant was previously developed by site-directed mutagenesis (*12*). All FNR variants were expressed in *E. coli* strain CodonPlus RIL (Stratagene); protein expression was induced with 125 μM IPTG at 30 °C for 4 h. After induction, cells were collected and the recombinant enzymes purified from cell extracts by affinity chromatography using Ni-NTA agarose (QIAGEN). Proteins were eluted with 100 mM imidazole and dialyzed against 50 mM Tris-HCl (pH 8.0) and 150 mM NaCl. The fusion proteins were digested with thrombin, and the Trx-His tag was removed by a second Ni-NTA affinity chromatographic procedure.

Recombinant pea Fd was expressed in *E. coli* using vector pET28-Fd (*21*) and purified essentially as described previously (*22*).

The purity of all protein preparations was assessed by sodium dodecyl sulfate−polyacrylamide gel electrophoresis (*23*), and protein concentrations were determined by UV−visible spectroscopy.

Spectral Analysis. Absorption spectra were recorded on a Shimadzu UV-2450 spectrophotometer at 25 °C. Samples were filtered through a G25 Sephadex (Sigma) spin column equilibrated with 50 mM Tris-HCl (pH 8.0) prior to measurements. Extinction coefficients of the FNR variants were determined by releasing FAD from the proteins by treatment with 0.2% (w/v) SDS and quantifying the flavin spectrophotometrically (*24*).

Determination of Dissociation Constants of the FNR−*Ligand Complexes*. The K_d values of the complexes between different FNR variants and the various compounds assayed were determined, unless otherwise stated, by difference absorption spectroscopy essentially as described previously (*13*). Solutions containing ~15 μM flavoprotein in 50 mM Tris-HCl (pH 8.0) were titrated at 25 °C with the ligands. After each addition, the absorbance spectrum (200−600 nm) was recorded. The difference spectra were then calculated, and the absorbance differences at the stated wavelengths were plotted against ligand concentration. When indicated, K_d values for the complexes between different FNR variants and the aromatic compounds were determined by protein fluorescence. FNR (20−30 μM) in

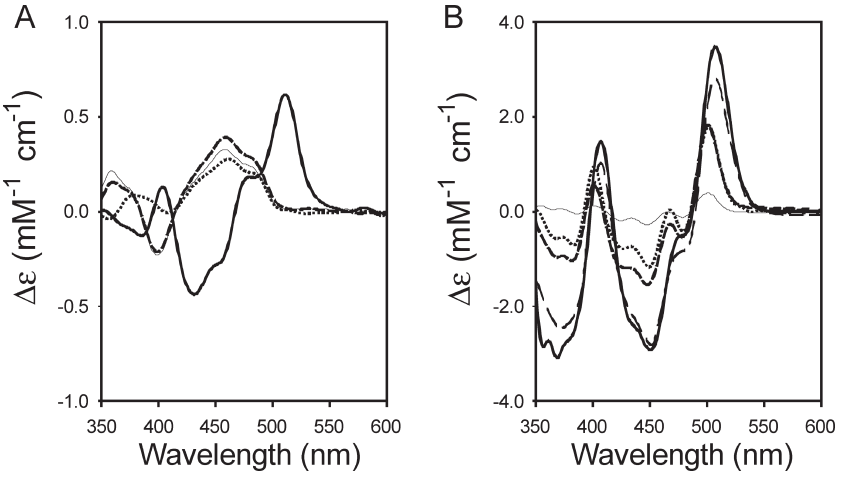

FIGURE 2: Spectroscopic characterization of the complexes between FNR and Y308S-FNR with $NADP^+$ and different analogues. Difference absorption spectra of the various complexes are shown for FNR (A) and Y308S-FNR (B): thick solid lines, $NADP^+$; long dashed lines, NAD^+; thin solid lines, 2′-P-AMP; dotted lines, nicotinamide; and short dashed lines, nicotinamide in the presence of saturating concentrations of 2′-P-AMP.

50 mM Tris-HCl (pH 8.0) was titrated at 25 °C with the different compounds. After each addition, flavin fluorescence (excitation at 456 nm and emission at 526 nm) was monitored using a Varian Cary Eclipse fluorescence spectrophotometer interfaced with a personal computer. Data were fitted to a theoretical equation for a 1:1 complex. In all cases, samples were previously filtered through a Sephadex G25 desalting column equilibrated with 50 mM Tris-HCl (pH 8.0).

Enzymatic Assays. FNR-dependent diaphorase was determined using published methods (*25*). All kinetic experiments were performed at 25 °C.

Determination of Parameters. All experimental data were fitted to theoretical curves using SIGMAPLOT (Systat Software Inc., Point Richmond, CA).

RESULTS

Interaction of $NADP^+$ and Different Analogues with FNR. Figure 2 shows the differential spectra elicited by the interaction of $NADP^+$, 2′-P-AMP, and nicotinamide with the wild-type and Y308S-FNR mutant enzymes under saturating conditions. The spectral alterations observed after mixing $NADP^+$ and FNR are shown in Figure 2A (thick solid line). Our data, which are coincident with published observations, show a positive differential signal at 510 nm that has been attributed to a stacking interaction of the nicotinamide with the isoalloxazine ring system of FAD (*6*, *9*). In contrast, the 2′-P-AMP−FNR differential spectrum shows a broad perturbation around 450 nm, and a small decrease at ~400 nm (Figure 2A, thin line), indicating that binding of a nucleotide at site P also alters the environment of the isoalloxazine (see Figure 1C). Interestingly, nicotinamide elicited a similar perturbation at 450 nm, but not at 400 nm (Figure 2A, dotted line). When nicotinamide was added to FNR in the presence of saturating concentrations of 2′-P-AMP, a similar differential spectrum with a broad peak at 470 nm was obtained (Figure 2A, dashed line).

In pea FNR, as well as in other flavoenzymes containing an FNR module, it has been extensively documented that a conserved aromatic side chain shields the isoalloxazine ring from solvent (*2*, *4*) (Sp1). This aromatic residue is in the putative position which the NADP(H) nicotinamide moiety should acquire during electron transfer (*9*). Replacement of the C-terminal Tyr of pea FNR with Ser generates a mutant enzyme with high affinity for $NADP^+$ (*6*, *10*). This enzyme can be expressed in *E. coli* and purified containing tightly bound $NADP^+$ (*6*). The nucleotide can then be removed by cibacron blue chromatography (*10*) and an enzyme free of $NADP^+$ thus prepared.

When the Y308S-FNR mutant was titrated with $NADP^+$, the differential spectrum elicited by the nucleotide displayed changes similar to, but greater in magnitude than, those observed with the wild-type enzyme (Figure 2B, thick solid line). At variance, only minor changes at 505 and 450 nm were detected with 2′-P-AMP. Spectra similar in shape but lower in magnitude versus those obtained with $NADP^+$ were detected when the enzyme was incubated with nicotinamide or 2′-P-AMP and nicotinamide. In the Y308S-FNR mutant, the absence of the terminal tyrosine may allow the free nicotinamide to enter site N and interact with the flavin in a manner similar to that of the $NADP^+$ nicotinamide moiety, thus producing detectable spectral changes in the 510 nm region. Together, our results indicate that the long wavelength spectral alterations observed when the enzyme is incubated with $NADP^+$ are mainly the result of interaction of the nicotinamide with the flavin.

Determination of the Affinity of the Complexes of FNR with Substrates and Analogues. We purified Y308S-FNR and the Y308S-FNR−$NADP^+$ complex and performed titrations with increasing concentrations of $NADP^+$ and different analogues (Sp2) to determine the affinity of both enzyme forms for these compounds; parallel experiments were conducted with FNR (Table 1). Y308S-FNR exhibited ~6 times more affinity for nicotinamide than the wild-type enzyme, indicating, as previously suggested, that the terminal tyrosine is directly involved in decreasing the affinity of the nicotinamide moiety of $NADP^+$ (Table 1, Sp3). Similarly, methyl-nicotinamide interacts with Y308S-FNR with an affinity of ~1 mM. In contrast, interaction of this compound with the wild-type enzyme was undetectable. The mutant enzyme containing $NADP^+$ displayed an increased K_d for 2′-P-AMP and nicotinamide relative to that of the Y308-FNR free enzyme. The bound $NADP^+$ interfered with binding of these analogues, an observation that can be taken as an indication that they interact with the same sites. Therefore, analogues should displace the nucleotide to interact with its binding site, and consequently, the pseudo-K_d values measured are higher than those observed for the $NADP^+$-free enzyme. No interaction was detected for the negatively

Table 1: Dissociation Constants of Mutant and Wild-Type FNRs for Fd, $NADP^+$, and Different Analogues

	enzyme form K_d[a] (μM)				
ligand	FNR	Y308S-FNR	Y308S-FNR−$NADP^+$	FNR−2′-P-AMP	Y308S-FNR−2′-P-AMP
$NADP^+$	7.5 ± 0.4	< 2	Nd[b]	Nd[b]	Nd[b]
NAD^+	UD[c]	190 ± 7[d]	Nd[b]	Nd[b]	Nd[b]
2′-P-AMP	14.4 ± 1.1	19.5 ± 1.7	614 ± 39	Nd[b]	Nd[b]
nicotinamide	23500 ± 2100	4000 ± 370	170000 ± 9000	400 ± 33	4000 ± 290
methyl-nicotinamide	> 200000[e]	1000 ± 90	> 200000	Nd[b]	Nd[b]
nicotinate	Nd[b]	> 200000	> 200000	> 200000	> 200000
ferredoxin	4.5 ± 0.3	0.8 ± 0.2	2.3 ± 0.4	Nd[b]	Nd[b]

[a] The K_d parameters were determined as described in Experimental Procedures. Absorbance difference data at 510 nm (FNR−$NADP^+$), 507 nm (Y308S-FNR−$NADP^+$), 503 nm (Y308S-FNR−NAD^+, Y308S-FNR−nicotinamide, Y308S-FNR−2′-P-AMP−nicotinamide, and Y308S-FNR−methyl-nicotinamide), 452 nm (FNR−2′-P-AMP, FNR−nicotinamide, and FNR−2′-P-AMP−nicotinamide), 505 nm (Y308S-FNR−2′-P-AMP, Y308S-FNR−$NADP^+$−2′-P-AMP), and 512 nm (Y308S-FNR−$NADP^+$−nicotinamide) were fitted to the theoretical equation for a 1:1 stoichiometric complex by means of nonlinear regression. Each parameter value represents the average of three independent experiments. [b] Not determined. [c] Undetectable. The K_d for the wild-type FNR−NAD^+ complex is too high to be measured with the methods employed (*6*). [d] From ref (*6*). [e] Indicates that K_d is equal or greater than this value and that it was not possible to measure it properly.

Table 2: Kinetic Constants of Wild-Type and Mutant FNRs for the Ferricyanide Diaphorase Reaction Using NADPH, NADH, and NMNH as Substrates[a]

enzyme	substrate	$[Fe(CN)_6^{3-}]$ (mM)	k_{cat} (s^{-1})	K_m (μM)	k_{esp}[b] (s^{-1} μM^{-1})	specificity[c] NADPH/NADH
FNR	NADPH	0.4	325 ± 50	17.0 ± 5.8	19.1 ± 9.4	21507
		1.0	300 ± 25	27.1 ± 4.2	11.1 ± 1.9	41123
	NADH	0.4	9.60 ± 0.55	10800 ± 1050	(8.89 ± 1.37) × 10^{-4}	
		1.0	13.9 ± 9.0	49100 ± 3050	(2.70 ± 1.91) × 10^{-4}	
	NMNH	1.0	< 0.001	Nd[d]	Nd[d]	
Y308S-FNR	NADPH	0.4	14.7 ± 0.5	< 0.5	> 29.4	> 65.2
		1.0	13.9 ± 0.7	< 0.5	> 27.9	> 182.6
	NADH	0.4	97.2 ± 3.4	215 ± 23	0.451 ± 0.064	
		1.0	108.0 ± 5.0	707 ± 86	0.153 ± 0.025	
	NMNH	1.0	1.8 ± 0.5	250 ± 9.0	0.022 ± 0.006	

[a] Potassium ferricyanide reduction was assessed using the diaphorase assay (*25*) in 50 mM Tris-HCl (pH 8.0). [b] $k_{esp} = k_{cat}/K_m$. [c] Specificity NADPH/NADH was determined as the ratio of k_{esp}(NADPH) to k_{esp}(NADH). [d] Not determined.

charged analogue, nicotinate, with any of the tested enzyme forms. We also measured the affinity of both enzymes for nicotinamide in the presence of saturating concentrations of 2′-P-AMP to determine if binding of this analogue to site P induces a change in the affinity for nicotinamide at site N. Interestingly, binding of 2′-P-AMP induced a 60-fold decrease in the K_d for nicotinamide in the wild-type enzyme. In contrast, this increase in affinity for nicotinamide induced by 2′-P-AMP was not detected in the mutant enzyme lacking the terminal tyrosine (Table 1).

The affinity for the protein substrate Fd was also investigated. We observed that the K_d for the Y308S-FNR−Fd complex was ~6-fold smaller than the K_d measured for the FNR−Fd complex. In contrast, the mutant enzyme containing bound $NADP^+$ exhibited a K_d for Fd 3-fold higher than that of the Y308S-FNR mutant free of $NADP^+$, but only 50% of that observed for the wild-type enzyme.

Determination of the Kinetic Constants of the Different Enzyme Forms. The kinetic parameters of the ferricyanide reductase activity of wild-type FNR and Y308S-FNR were assayed under the same conditions for NADPH and NADH using two different ferricyanide concentrations (Table 2). As previously reported, the wild-type enzyme displayed a strong preference for NADPH over NADH (*6*). Interestingly, the ferricyanide concentration did not significantly affect the k_{cat} values for either enzyme form, but it did influence the K_m for the nucleotidic substrate. A kinetic analysis of the observed effect indicates that ferricyanide acts as a competitive inhibitor of both NADPH and NADH, in addition to its role as a substrate (data not shown). Likewise, we determined that 2′-P-AMP behaves as a competitive inhibitor for NADPH on the diaphorase reaction (Sp4). The inhibition constants (K_i) were practically identical for wild-type FNR (30.4 ± 2.9 μM) and Y308S-FNR (30.7 ± 3.4 μM). We then tested if the reduced nicotinamide mononucleotide (NMNH) could act as a substrate of the different enzyme forms. NMNH lacks the 2′-P-AMP moiety present in NADPH. The mutant enzyme was able to catalyze the oxidation of NMNH at low rates, but no activity was observed with the wild-type enzyme.

Effect of Aromatic Compounds on the Activity of the Different Enzyme Forms. We investigated the effect of several aromatic compounds, most of them structurally related to tyrosine or nicotinamide, on the catalytic properties of wild-type FNR and Y308S-FNR. The rationale for these experiments is based on the previously proposed hypothesis (*2*, *7*) that the terminal tyrosine is in equilibrium between "in" and "out" conformations when NADP(H) is bound to the enzyme. The out conformation is the one with the nicotinamide in the proper position and, then, the catalytically competent species. In contrast, the in conformation has the tyrosine facing the flavin ring and the nicotinamide in a nonproductive position. This equilibrium should proceed on a short time scale so as not to be rate-limiting, as was previously suggested (*4*, *8*). If this hypothesis is correct, the tyrosine function could be properly replaced by other appropriate aromatic compounds, provided that they interact with the catalytic site and a sufficient concentration is present in the reaction medium. We evaluated the effects on diaphorase

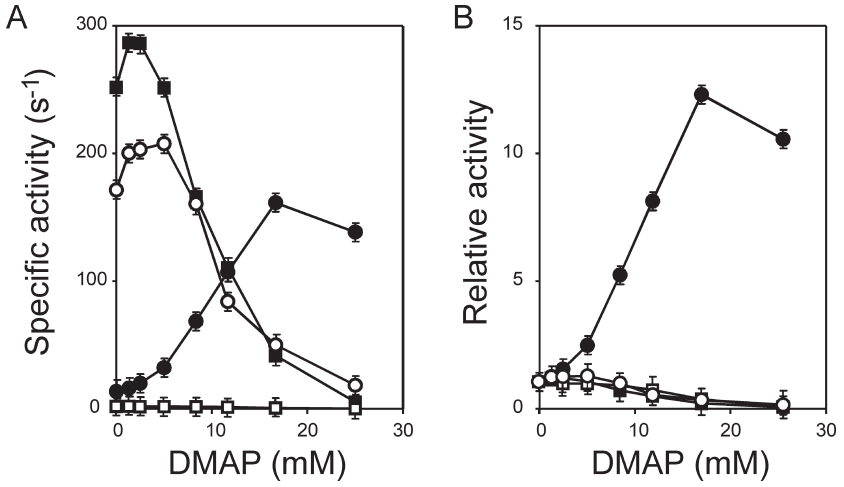

FIGURE 3: Effect of DMAP on the diaphorase activity of wild-type FNR and Y308S-FNR. The NADPH-dependent (black symbols) and NADH-dependent (white symbols) ferricyanide diaphorase activities were assayed in the presence of increasing DMAP concentrations (0−25 mM), using wild-type FNR (squares) and Y308S-FNR (circles): (A) diaphorase activity and (B) relative activity (the ratio between activity in the presence of DMAP to activity in the absence of the compound) plotted as a function of DMAP concentration.

activity of nicotinamide, pyridine, nicotinic acid, morpholine, piperidine, 4-hydroxyphenylglycine, tryptophan, imidazole, and DMAP (see the structures in Sp2). DMAP displayed the strongest effect on both enzyme forms. Pyridine and morpholine also altered the enzymatic activity. Negligible effects were detected with piperidine and nicotinic acid (data not shown). At low concentrations (1−5 mM), DMAP exerted an activating effect on both NADPH- and NADH-dependent diaphorase activities of the wild-type and Y308S-FNR enzymes, respectively (Figure 3A), but as the concentration of DMAP was increased, the alteration generated by the replacement of Y308 with a serine was progressively reverted (Figure 3A). In the presence of this compound, the NADPH-dependent diaphorase activity of the mutant Y308S-FNR increased ~12-fold [Figure 3A,B (●)], whereas the NADH-dependent diaphorase activity decreased to levels similar to those of the wild-type enzyme.

Interaction of Aromatic Compounds with the Different FNR Forms. Addition of DMAP elicited very weak spectral changes in wild-type FNR. In contrast, it induced detectable changes in the intrinsic FAD fluorescence of FNR. These observations can be taken as an indication that the aromatic ring of Y308 is being replaced by the compound upon interaction with the enzyme. Then, we performed titrations with increasing concentrations of DMAP and other aromatic compounds to determine the affinity of the different enzyme forms for these molecules (Table 3). Enzyme activation by DMAP was observed between 0 and 5 mM which is in agreement with the affinities determined by enzyme intrinsic fluorescence. At these concentrations, the aromatic compounds probably competed with the NADPH nicotinamide for the proper position on the catalytic site favoring product release. It is worth recalling that at full occupancy of site P by $NADP^+$, only ~16% of site N is occupied by the nicotinamide displacing the tyrosine (*6*). Thus, when the effect of DMAP is exerted, a complex equilibrium among the enzyme, the NADP(H) nicotinamide, and the DMAP probably occurs.

When the Y308S-FNR mutant protein was incubated with DMAP, the spectral changes included two minima (385 and 438 nm) and a maximum at 496 nm (Figure 4A). This differential spectrum is quite similar to the one obtained with nicotinamide and $NADP^+$ (compare Figures 2B and 4A), although it is slightly shifted toward shorter wavelengths, suggesting that a similar interaction with the flavin is taking place with the nucleotide and the aromatic compound tested.

Table 3: Dissociation Constants of Mutant and Wild-Type FNRs for Different Aromatic Compounds

	enzyme form K_d[a] (μM)		
ligand	FNR	Y308S-FNR−$NADP^+$	FNR−2′-P-AMP
DMAP	357.4 ± 18.3	Nd[b]	251.1 ± 20.7
imidazole	367.0 ± 40.2	120.0 ± 7.41	228.9 ± 25.6
4-OH-phenyl glycine	417.0 ± 14.6	133.2 ± 12.7	336.8 ± 15.8
tryptophan	221.8 ± 20.2	119.0 ± 10.3	128.3 ± 11.4

[a] The K_d parameters were determined by spectrofluorometric titrations of the selected FNR forms with the indicated organic compound as described in Experimental Procedures. Each parameter value represents the average of three independent experiments. [b] Not determined.

Titration of the Y308S-FNR−$NADP^+$ complex with DMAP (Figure 4C) produced spectral perturbations at 507 nm which were similar but opposite in sign to those elicited by the Y308S-FNR form upon $NADP^+$ binding (Figure 2B), consistent with the loss of the $NADP^+$ nicotinamide stacking on the flavin. This effect correlates with the activation of the NADPH diaphorase activity of the enzyme, which showed a maximal increase at 17 mM DMAP (see Figure 3B).

The interaction of DMAP with both enzyme variants was studied in more detail. It can be argued that DMAP could interact also with site P, thereby influencing the affinity of the enzyme for DMAP on site N, as in the case of 2′-P-AMP with free nicotinamide binding. To rule out this possibility, we determined the K_d values of the wild-type FNR−$NADP^+$ complex in the presence of different concentrations of DMAP. As shown in Figure 5, the spectral changes elicited by $NADP^+$ on the enzyme are similar in shape but lower in amplitude. Interestingly, the K_d values for $NADP^+$ obtained in the presence of 3 and 50 mM DMAP were 8.9 ± 0.9 and 9.6 ± 1.3 μM, respectively, fairly similar to the one determined in the absence of the organic compound (7.5 ± 0.4 μM) (inset of Figure 5). It is known that in wild-type FNR, the enzyme−$NADP^+$ complex is mainly stabilized by interactions involving the 2′-P-AMP moiety of the dinucleotide, whereas the nicotinamide ring does not contribute

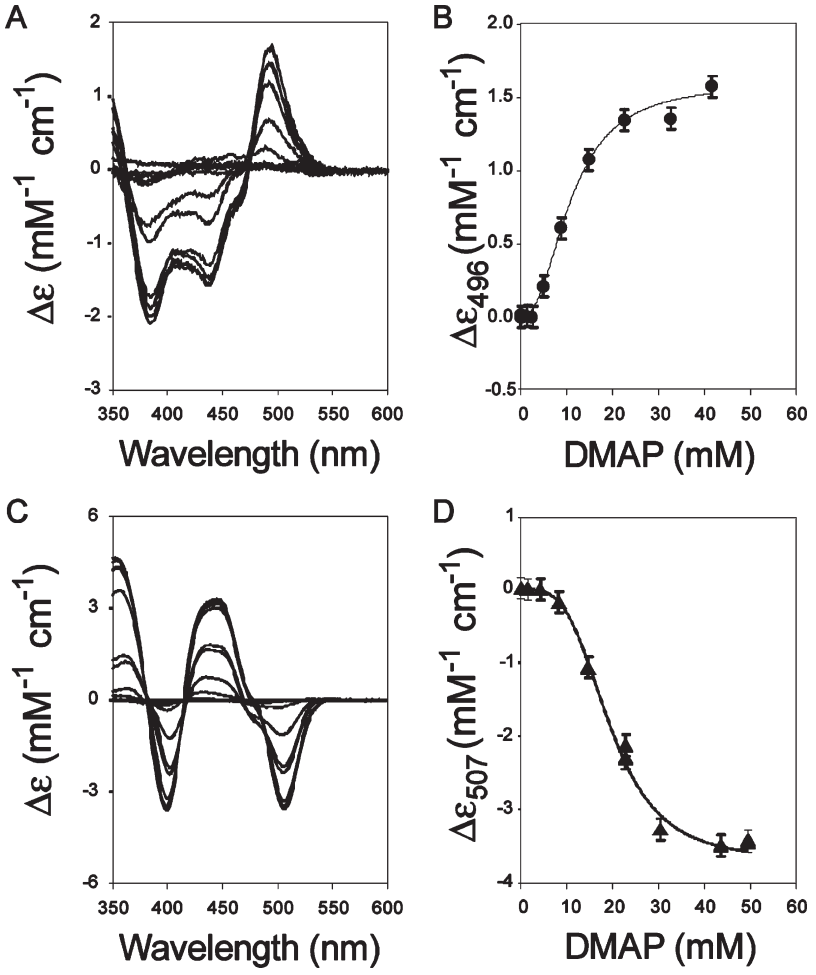

FIGURE 4: Spectroscopic characterization of the Y308S-FNR−DMAP and Y308S-FNR−$NADP^+$−DMAP complexes. Difference absorption spectra elicited by the addition of increasing concentrations of DMAP are shown for Y308S-FNR (A) and the Y308S-FNR−$NADP^+$ complex (C). Panels B and D represent the change in $\Delta\varepsilon$ at 496 and 507 nm, respectively, for the Y308S-FNR and Y308S-FNR−$NADP^+$ enzymes as a function of DMAP concentration.

significantly to the binding energy (*16*). Taken together, our results indicate that DMAP is influencing the interaction of the nicotinamide at site N but not the interaction of the coenzyme at site P. To further support our hypothesis, we analyzed the effect of 2′-P-AMP on the enzymatic activity of both enzyme forms in the presence of DMAP. As shown in Table 4, the effect of 2′-P-AMP on both enzymes is the same in the absence or presence of DMAP, thus ruling out the possibility that both compounds are competing for site P.

DISCUSSION

The research described here was undertaken with the aim of identifying the mechanisms by which plastidic-type FNRs achieve their high catalytic efficiency and strong preference for NADP(H) over NAD(H). One of the key issues in the FNR catalytic mechanism is the manner in which the NADP(H) nicotinamide enters the catalytic site and properly binds to it. During productive binding, N5 of the flavin and C4 of the nicotinamide rings are aligned for hydride transfer (*9*). This arrangement is essential for efficient electron and hydride transfer (*26*). The analysis of the different FNR crystal structures already available shows that the outer face of the flavin is partially shielded from solvent. This role is carried out by an aromatic amino acid in plastidic FNRs and in subclass II bacterial FNRs or by an alanine in subclass I bacterial FNRs (*1*, *2*) and references therein. In contrast, crystal structures of

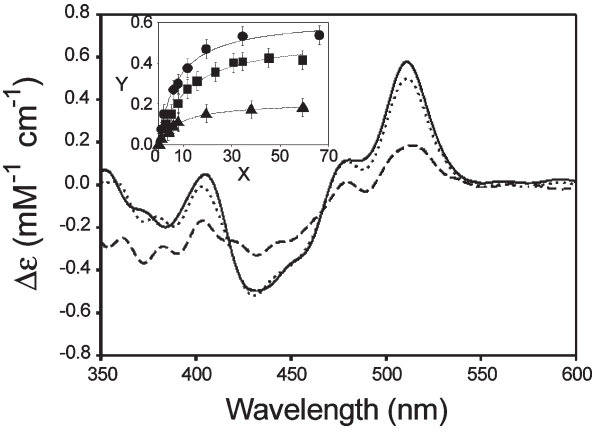

FIGURE 5: Spectroscopic characterization of the complexes between FNR and $NADP^+$ in the presence of DMAP. Difference absorption spectra are shown for the various FNR−$NADP^+$ complexes in the absence or presence of DMAP: thick solid line, $NADP^+$ without DMAP; dotted line, $NADP^+$ with 3 mM DMAP; and dashed line, $NADP^+$ with 50 mM DMAP. The inset depicts difference absorption data fitted to the theoretical equation for a 1:1 complex by means of nonlinear regression with $\Delta\varepsilon_{510}$ (mM^{-1} cm^{-1}) values on the *y*-axis and $NADP^+$ (μM) concentration on the *x*-axis: (●) $NADP^+$ without DMAP (K_d = 7.5 ± 0.4 μM), (■) $NADP^+$ with 3 mM DMAP (K_d = 8.9 ± 0.9 μM), and (▲) $NADP^+$ with 50 mM DMAP (K_d = 9.6 ± 1.3 μM).

FNR containing bound $NADP^+$ (*3*, *9*, *18*, *27*, *28*) indicate that during binding of the nucleotide, the terminal amino acid should be removed from the flavin face to allow the nicotinamide to be

Table 4: Effect of 2′-P-AMP on the Enzymatic Activity of Mutant and Wild-Type FNRs in the Presence of DMAP

	enzymatic activity[a] (s^{-1})			
enzyme	control	2′-P-AMP	DMAP	2′-P-AMP/DMAP
FNR	262.0 ± 12.1	230.6 ± 18.7	41.5 ± 4.2	39.5 ± 2.5
Y308S-FNR	13.5 ± 1.4	11.9 ± 0.8	161.4 ± 13.1	37.2 ± 3.2

[a] Diaphorase activity was determined as described in Experimental Procedures using 25 nM wild-type FNR or 100 nM Y308S-FNR, 100 μM NADPH, and 1 mM potassium ferricyanide. DMAP and 2′-P-AMP, when present, were at concentrations of 17 mM and 30 μM, respectively. Each parameter value represents the average of three independent experiments.

docked in the productive position (*9*). Experimental evidence indicates that interaction between the nicotinamide of $NADP^+$ and the isoalloxazine is modulated by the terminal tyrosine (Y308 in pea FNR) (*6*, *7*, *10*); evolution has probably adjusted this interaction precisely to optimize catalysis (*8*). This exchange between the Y308 side chain and the $NADP^+$ nicotinamide has been experimentally demonstrated to be the rate-limiting step during turnover (*7*). Consequently, the mobility of this amino acid has been shown to be essential for obtaining high catalytic rates (*13*).

Several conclusions can thus be drawn from our study. The interaction of the enzyme with $NADP^+$ is mainly governed by the 2′-P-AMP portion of the nucleotide, as previously reported (*6*). Interestingly, interaction of the terminal tyrosine with the flavin did not affect 2′-P-AMP binding, as shown by the fact that K_d values for this analogue are similar when the wild-type and mutant enzymes were tested. In contrast, nicotinamide binding was strongly affected by the terminal tyrosine. The wild-type enzyme displayed a low affinity for nicotinamide (Table 1); consequently, no reaction was observed using NMNH (Table 2). In contrast, the mutant enzyme lacking the terminal tyrosine exhibited a 6-fold increase in its affinity for nicotinamide and significant activity with NMNH (Tables 1 and 2). Free NMNH constitutes one-half of the NADPH molecule, lacking the adenosine moiety which is the major determinant for NADPH binding. The nicotinamide moiety of free NMNH is identical to the one found in NADPH. It is therefore reasonable to assume that free NMNH reaction will follow the same hydride transfer mechanism that has been proposed for NADPH oxidation by FNR (*6*).

As previously suggested, the strong preference for NADP(H) over NAD(H) in the FNR enzyme family is achieved by specific contacts with characteristic functional groups of each substrate (the 2′-phosphate or the 2′-OH of the adenosine ribose). Y308 contributes to this discrimination by weakening the interactions of the enzyme with traits common to both nucleotides, such as the nicotinamide ring (*6*, *10*). A similar observation was made for the flavocytochrome P450 BM3 from *Bacillus megaterium* (*29*). Thus, in Y308S-FNR, where the effect of the terminal tyrosine is lost, the increase in the catalytic efficiencies for NADH oxidation relative to wild-type FNR is due to the simultaneous increase in k_{cat} and decrease in K_m. The lower affinity for NADH compared to that for NADPH exhibited by the mutant FNR prevents product release from becoming rate-limiting, and thus from negatively affecting k_{cat} (refs (*4*), (*6*), and (*7*) and this work). Other residues, in addition to the terminal tyrosine, are involved in determining enzyme specificity (*3*, *4*), probably acting in concert to improve discrimination against NAD(H). It remains unclear how the high turnover rates are obtained with such a low affinity of the enzyme for nicotinamide. In this study, we found that binding of 2′-P-AMP increased the affinity of the enzyme for free nicotinamide 60-fold (Table 1). Thus, during enzyme turnover, when the 2′-P-AMP part of $NADP^+$ is bound to site P, a conformational change is produced in the reductase that favors binding of the nicotinamide moiety of $NADP^+$ to site N, thereby promoting enzyme turnover. This conformational change may be inferred by the spectral alterations observed when 2′-P-AMP binds to FNR (see Figure 2), which indicates that binding of a nucleotide at site P alters the environment of the flavin, located at site N. The loop including C266, G267, and L268 undergoes a structural rearrangement upon $NADP^+$ binding (*18*); L268, which is close to $NADP^+$ when the nucleotide is bound to the enzyme, may trigger the process. We have previously observed that C266, G267, and L268 are involved in fine-tuning the interaction of the tyrosine with the flavin, consequently affecting binding of the nicotinamide portion of $NADP^+$ to the catalytic site (*8*). It has been proposed that in *Anabaena* FNR the 261−265 loop (equivalent to the 266−270 region in pea FNR) is involved in determining coenzyme specificity (*4*). A T155G/A160T/L263P triple mutant led to a marked retraction of the above-mentioned loop, a decrease in enzyme catalytic efficiency, and a relaxation of enzyme specificity. Experimental data indicate that when $NADP^+$ is present at saturating concentrations, the degree of nicotinamide ring occupancy of the binding site is ~14−15%, as revealed by the extinction coefficient values of the peak near 510 nm in difference spectra elicited by pyridine nucleotide binding to the various pea FNR forms (*6*). Taking into account this degree of occupancy as well as the corresponding dissociation constants for $NADP^+$ and analogues (Table 1), we could simulate the equilibrium for the two halves of NADP(H). On the basis of these assumptions, we infer that if site P is empty (then K_d for free nicotinamide changes from 400 to 23500 μM) an ~50-fold decrease in site N occupancy should result. The above-mentioned values indicate that occupancy of site N, where hydride transfers occurs, decreases from 15 to 0.3%. Consequently, the affinity of the nicotinamide portion of $NADP^+$ for site N when site P is occupied is increased to optimize catalytic rates; this probably still allows for rapid release of the product or even facilitation of product release.

DMAP inhibited wild-type FNR with NADPH or NADH as the substrate and Y308S-FNR with NADH as the substrate. Instead, it activated Y308S-FNR with NADPH as the substrate. Since the latter is the only case in which product dissociation is rate-determining (*4*), it is reasonable to assume that DMAP induces product release. As this is a kinetic effect, presumably a simple inhibitor would not have such an effect, suggesting that the main role of Y308 is to weaken the isoalloxazine−nicotinamide interaction, therefore inducing product release and increasing the reaction rate of the enzyme. A similar observation has been made in neuronal nitric oxide synthase, an enzyme that contains a FAD/NADPH subdomain which belongs to the FNR structural family (*30*). In this synthase, a phenylalanine prevents nucleotide release from being rate-limiting, modulating a conformational equilibrium which controls transfer of an electron from NADPH/FAD to the other subdomain that contains FMN. Recently, Wang et al. (*28*) determined by X-ray crystallography and nuclear magnetic resonance that the surface of the FNR from *Pseudomonas aeruginosa*, a typical bacterial-type FNR with low catalytic efficiency, has a preformed cavity where the cofactor binds to form the enzyme−$NADP^+$ complex with

minimal perturbation of the protein structure. These authors suggested that formation of a productive complex in the bacterial enzyme occurs in a time frame (micro- to milliseconds) that is detrimental to catalytic competence (*28*). Our results, in contrast, clearly demonstrate that during nucleotide binding to plastidic-type FNRs, improvement of substrate interaction and catalysis is due to a classical induced-fit mechanism, as postulated by Koshland (*19*). These mechanistic differences may explain the dramatic increase in the catalytic efficiency of the plastidic reductases over those of their bacterial counterparts.

Tyrosine 308 may have several functions in FNR catalytic activity. One might be to close the catalytic site, thereby modulating entry of nicotinamide into site N. It might also protect the flavin by shielding it from the environment [as experimentally demonstrated by a number of methods (refs (*2*), (*9*), and (*10*) and references therein) (Sp1)]. Our results support the idea that the terminal tyrosine R group freely equilibrates between the in and out conformations and that in the presence of NADP(H), the nicotinamide reaches an equilibrium which optimizes catalytic turnover. All available experimental data indicate that overall interactions between flavin and Y308 are attractive (*4*, *6*, *8*, *9*) and mainly driven by the aromatic character of both molecules. The near coplanar orientation of the phenol ring of Y308 with the flavin provides very strong $\pi-\pi$ interactions, and repulsive interactions should be negligible. Indeed, removal of the favorable interactions via replacement of the tyrosine with a serine causes an energy change of ~1.9 kcal/mol in the stability of the protein (*11*). Our observations indicate that if the proper aromatic compound is employed, the absence of the terminal tyrosine could be simulated by increasing the concentration of this compound. This observation can be taken as a clear indication of the existence of an equilibrium involving the aromatic compound and the nicotinamide. The capability of nucleotide discrimination was probably initially acquired by using aromatic compounds from the environment and then subsequently evolutionarily selected for. Thus, nicotinamide will interact with the flavin by selection from a "*carte du jour*" of preexisting different conformations. This mechanism can be interpreted as the one postulated by Monod et al. (*20*) for allosteric transitions, and then interpreted in a more detailed manner by Tsai et al. (*31*). These authors have suggested that several protein species whose energy minima are separated by small energy barriers may exist. The protein conformational diversity is great, and the conformers binding to cofactors or ligands may be different from those found in crystal structures, as is the case for all FNR proteins crystallized to date with bound $NADP^+$ (*9*, *18*, *27*, *28*, *32*). In this model, the proper position of the substrate (in this case the nicotinamide of $NADP^+$) could be obtained with only one of the conformers which is neither in an energy minimum nor represented in the deduced crystal structure. The movement of tyrosines interacting with flavins has been documented by several techniques. Using single-molecule electron transfer in *E. coli* flavin reductase, a conformational fluctuation at multiple time scales was observed between the flavin and the interacting tyrosine (*33*). Employing fluorescence depolarization and detection of the direction of the emission of the *E. coli* glutathione reductase FAD fluorescence, van den Berg et al. elucidated a mechanism in which $NADP^+$ intercalates its structure between the flavin and tyrosine as a clear indication of a tyrosine−flavin rearrangement (*34*). By means of the same system used for *E. coli* glutathione reductase, the fluorescence lifetime spectra of FNR yielded just a single decay component at the limit of detection (~3 ps), which indicates that there is a fast movement of the flavin−tyrosine arrangement on the subpicosecond time scale (*35*).

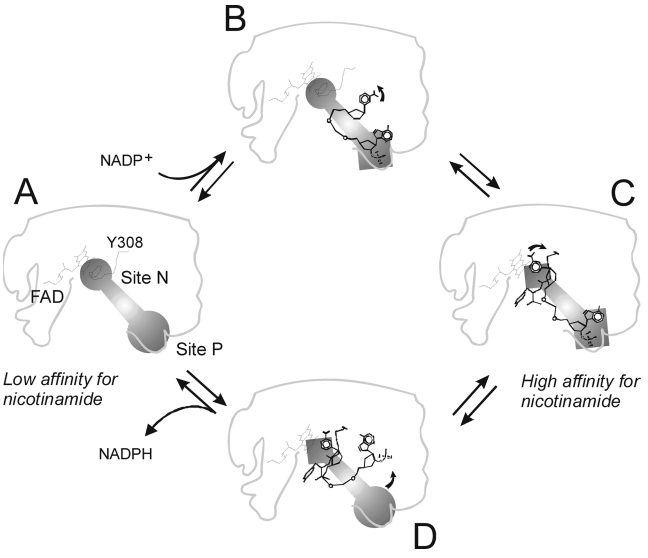

FIGURE 6: Schematic representation of the induced-fit and equilibrium dynamics mode of binding of NADP(H) to FNR. Sites N and P are represented as circles when they are in their native states and as squares after undergoing a conformational change. (A) Free enzyme in solution. (B) Conformational change induced in site P by binding of the 2′-P-AMP moiety of $NADP^+$. (C) Conformational change at site N as a consequence of binding the 2′-P-AMP moiety of $NADP^+$ at site P, which allows nicotinamide binding. (D) Substrate release and return of the enzyme to the initial conformation. Details are provided in the text.

Taking into account the available data, we propose the following model. Discrimination against NAD(H) is accomplished by inhibiting nicotinamide binding. An equilibrium is established in which the conformation with the Y308 side chain stacked on the *re*-face of the flavin is highly populated. Virtually no nicotinamide interacts with the catalytic site at physiological nucleotide concentrations (Figure 6A,B, circular site N). Binding of NADP(H) at site P produces a conformational change (Figure 6B, squared site P) which favors docking of nicotinamide to site N through weakening of the interaction between the tyrosine and the flavin (Figure 6C, squared site N). Since this exchange is produced by a rapid equilibrium, the substrate is not impeded from leaving the catalytic site. As soon as site P is empty, reversal of the conformational change forces the nicotinamide out of site N (Figure 6D).

ACKNOWLEDGMENT

E.A.C. and N.C. are staff members of the Consejo Nacional de Investigaciones Científicas y Técnicas (CONICET, Argentina). D.H.P. and M.A.M. are fellows of the same institution.

SUPPORTING INFORMATION AVAILABLE

Spectroscopic characterization of the complexes between Y308S-FNR and nicotinamide and the structures of nucleotides and analogues used. This material is available free of charge via the Internet at http://pubs.acs.org.

REFERENCES

1. Ceccarelli, E. A., Arakaki, A. K., Cortez, N., and Carrillo, N. (2004) Functional plasticity and catalytic efficiency in plant and bacterial ferredoxin-NADP(H) reductases. *Biochim. Biophys. Acta 1698*, 155–165.

2. Carrillo, N., and Ceccarelli, E. A. (2003) Open questions in ferredoxin-NADP$^+$ reductase catalytic mechanism. *Eur. J. Biochem. 270*, 1900–1915.
3. Medina, M., Luquita, A., Tejero, J., Hermoso, J., Mayoral, T., Sanz-Aparicio, J., Grever, K., and Gomez-Moreno, C. (2001) Probing the determinants of coenzyme specificity in ferredoxin-NADP$^+$ reductase by site-directed mutagenesis. *J. Biol. Chem. 276*, 11902–11912.
4. Tejero, J., Martinez-Julvez, M., Mayoral, T., Luquita, A., Sanz-Aparicio, J., Hermoso, J. A., Hurley, J. K., Tollin, G., Gomez-Moreno, C., and Medina, M. (2003) Involvement of the pyrophosphate and the 2′-phosphate binding regions of ferredoxin-NADP$^+$ reductase in coenzyme specificity. *J. Biol. Chem. 278*, 49203–49214.
5. Karplus, P. A., and Bruns, C. M. (1994) Structure-function relations for ferredoxin reductase. *J. Bioenerg. Biomembr. 26*, 89–99.
6. Piubelli, L., Aliverti, A., Arakaki, A. K., Carrillo, N., Ceccarelli, E. A., Karplus, P. A., and Zanetti, G. (2000) Competition between C-terminal tyrosine and nicotinamide modulates pyridine nucleotide affinity and specificity in plant ferredoxin- NADP$^+$ reductase. *J. Biol. Chem. 275*, 10472–10476.
7. Tejero, J., Perez-Dorado, I., Maya, C., Martinez-Julvez, M., Sanz-Aparicio, J., Gomez-Moreno, C., Hermoso, J. A., and Medina, M. (2005) C-Terminal tyrosine of ferredoxin-NADP$^+$ reductase in hydride transfer processes with NAD(P)$^+$/H. *Biochemistry 44*, 13477–13490.
8. Musumeci, M. A., Arakaki, A. K., Rial, D. V., Catalano-Dupuy, D. L., and Ceccarelli, E. A. (2008) Modulation of the enzymatic efficiency of ferredoxin-NADP(H) reductase by the amino acid volume around the catalytic site. *FEBS J. 275*, 1350–1366.
9. Deng, Z., Aliverti, A., Zanetti, G., Arakaki, A. K., Ottado, J., Orellano, E. G., Calcaterra, N. B., Ceccarelli, E. A., Carrillo, N., and Karplus, P. A. (1999) A productive NADP$^+$ binding mode of ferredoxin-NADP + reductase revealed by protein engineering and crystallographic studies. *Nat. Struct. Biol. 6*, 847–853.
10. Nogues, I., Tejero, J., Hurley, J. K., Paladini, D., Frago, S., Tollin, G., Mayhew, S. G., Gomez-Moreno, C., Ceccarelli, E. A., Carrillo, N., and Medina, M. (2004) Role of the C-terminal tyrosine of ferredoxin-nicotinamide adenine dinucleotide phosphate reductase in the electron transfer processes with its protein partners ferredoxin and flavodoxin. *Biochemistry 43*, 6127–6137.
11. Calcaterra, N. B., Pico, G. A., Orellano, E. G., Ottado, J., Carrillo, N., and Ceccarelli, E. A. (1995) Contribution of the FAD binding site residue tyrosine 308 to the stability of pea ferredoxin-NADP$^+$ oxidoreductase. *Biochemistry 34*, 12842–12848.
12. Orellano, E. G., Calcaterra, N. B., Carrillo, N., and Ceccarelli, E. A. (1993) Probing the role of the carboxyl-terminal region of ferredoxin-NADP$^+$ reductase by site-directed mutagenesis and deletion analysis. *J. Biol. Chem. 268*, 19267–19273.
13. Catalano-Dupuy, D. L., Orecchia, M., Rial, D. V., and Ceccarelli, E. A. (2006) Reduction of the pea ferredoxin-NADP(H) reductase catalytic efficiency by the structuring of a carboxyl-terminal artificial metal binding site. *Biochemistry 45*, 13899–13909.
14. Maeda, M., Lee, Y. H., Ikegami, T., Tamura, K., Hoshino, M., Yamazaki, T., Nakayama, M., Hase, T., and Goto, Y. (2005) Identification of the N- and C-terminal substrate binding segments of ferredoxin-NADP$^+$ reductase by NMR. *Biochemistry 44*, 10644–10653.
15. Batie, C. J., and Kamin, H. (1984) Electron transfer by ferredoxin: NADP$^+$ reductase. Rapid-reaction evidence for participation of a ternary complex. *J. Biol. Chem. 259*, 11976–11985.
16. Batie, C. J., and Kamin, H. (1986) Association of ferredoxin-NADP$^+$ reductase with NADP(H): Specificity and oxidation-reduction properties. *J. Biol. Chem. 261*, 11214–11223.
17. Kurisu, G., Kusunoki, M., Katoh, E., Yamazaki, T., Teshima, K., Onda, Y., Kimata-Ariga, Y., and Hase, T. (2001) Structure of the electron transfer complex between ferredoxin and ferredoxin-NADP$^+$ reductase. *Nat. Struct. Biol. 8*, 117–121.
18. Hermoso, J. A., Mayoral, T., Faro, M., Gomez-Moreno, C., Sanz-Aparicio, J., and Medina, M. (2002) Mechanism of coenzyme recognition and binding revealed by crystal structure analysis of ferredoxin-NADP$^+$ reductase complexed with NADP$^+$. *J. Mol. Biol. 319*, 1133–1142.
19. Koshland, D. E. (1958) Application of a theory of enzyme specificity to protein synthesis. *Proc. Natl. Acad. Sci. U.S.A. 44*, 98–104.
20. Monod, J., Wyman, J., and Changeux, J. P. (1965) On the nature of allosteric transitions: A plausible model. *J. Mol. Biol. 12*, 88–118.
21. Catalano Dupuy, D. L., Rial, D. V., and Ceccarelli, E. A. (2004) Inhibition of pea ferredoxin-NADP(H) reductase by Zn-ferrocyanide. *Eur. J. Biochem. 271*, 4582–4593.
22. Hurley, J. K., Salamon, Z., Meyer, T. E., Fitch, J. C., Cusanovich, M. A., Markley, J. L., Cheng, H., Xia, B., Chae, Y. K., and Medina, M. (1993) Amino acid residues in *Anabaena* ferredoxin crucial to interaction with ferredoxin-NADP$^+$ reductase: Site-directed mutagenesis and laser flash photolysis. *Biochemistry 32*, 9346–9354.
23. Laemmli, U. K. (1970) Cleavage of structural proteins during the assembly of the head of bacteriophage T4. *Nature 227*, 680–685.
24. Aliverti, A., Bruns, C. M., Pandini, V. E., Karplus, P. A., Vanoni, M. A., Curti, B., and Zanetti, G. (1995) Involvement of serine 96 in the catalytic mechanism of ferredoxin-NADP$^+$ reductase: Structure−function relationship as studied by site-directed mutagenesis and X-ray crystallography. *Biochemistry 34*, 8371–8379.
25. Zanetti, G. (1976) A lysyl residue at the NADP$^+$ binding site of ferredoxin-NADP$^+$ reductase. *Biochim. Biophys. Acta 445*, 14–24.
26. Ortiz-Maldonado, M., Entsch, B., and Ballou, D. P. (2003) Conformational changes combined with charge-transfer interactions are essential for reduction in catalysis by p-hydroxybenzoate hydroxylase. *Biochemistry 42*, 11234–11242.
27. Nogues, I., Perez-Dorado, I., Frago, S., Bittel, C., Mayhew, S. G., Gomez-Moreno, C., Hermoso, J. A., Medina, M., Cortez, N., and Carrillo, N. (2005) The ferredoxin-NADP(H) reductase from *Rhodobacter capsulatus*: Molecular structure and catalytic mechanism. *Biochemistry 44*, 11730–11740.
28. Wang, A., Rodriguez, J. C., Han, H., Schonbrunn, E., and Rivera, M. (2008) X-ray crystallographic and solution state nuclear magnetic resonance spectroscopic investigations of NADP$^+$ binding to ferredoxin-NADP$^+$ reductase from *Pseudomonas aeruginosa*. *Biochemistry 47*, 8080–8093.
29. Neeli, R., Roitel, O., Scrutton, N. S., and Munro, A. W. (2005) Switching pyridine nucleotide specificity in P450 BM3: Mechanistic analysis of the W1046H and W1046A enzymes. *J. Biol. Chem. 280*, 17634–17644.
30. Konas, D. W., Zhu, K., Sharma, M., Aulak, K. S., Brudvig, G. W., and Stuehr, D. J. (2004) The FAD-shielding residue Phe1395 regulates neuronal nitric-oxide synthase catalysis by controlling NADP$^+$ affinity and a conformational equilibrium within the flavoprotein domain. *J. Biol. Chem. 279*, 35412–35425.
31. Tsai, C. J., Kumar, S., Ma, B., and Nussinov, R. (1999) Folding funnels, binding funnels, and protein function. *Protein Sci. 8*, 1181–1190.
32. Mayoral, T., Martinez-Julvez, M., Perez-Dorado, I., Sanz-Aparicio, J., Gomez-Moreno, C., Medina, M., and Hermoso, J. A. (2005) Structural analysis of interactions for complex formation between ferredoxin-NADP$^+$ reductase and its protein partners. *Proteins 59*, 592–602.
33. Yang, H., Luo, G., Karnchanaphanurach, P., Louie, T. M., Rech, I., Cova, S., Xun, L., and Xie, X. S. (2003) Protein conformational dynamics probed by single-molecule electron transfer. *Science 302*, 262–266.
34. van den Berg, P. A., van Hoek, A., and Visser, A. J. (2004) Evidence for a novel mechanism of time-resolved flavin fluorescence depolarization in glutathione reductase. *Biophys. J. 87*, 2577–2586.
35. van den Berg, P. A. W., and Visser, A. J. W. G. (2001) Tracking molecular dynamics of flavoproteins with time-resolved fluorescence spectroscopy. In New Trends in Fluorescence Spectroscopy: Applications to Chemical and Life Sciences (Valeur, B., and Brochon, J.-C., Eds.) pp 457−486, Springer, Berlin.